ANESTHESIOLOGY

Static and Dynamic Transpulmonary Driving Pressures Affect Lung and Diaphragm Injury during Pressure-controlled *versus* Pressure-support Ventilation in Experimental Mild Lung Injury in Rats

Eliete F. Pinto, M.Sc., Raquel S. Santos, Ph.D., Mariana A. Antunes, Ph.D., Ligia A. Maia, Ph.D., Gisele A. Padilha, Ph.D., Joana de A. Machado, M.S., Anna C. F. Carvalho, M.S., Marcos V. S. Fernandes, M.S., Vera L. Capelozzi, M.D., Ph.D., Marcelo Gama de Abreu, M.D., Ph.D., Paolo Pelosi, M.D., F.E.R.S., Patricia R. M. Rocco, M.D., Ph.D., Pedro L. Silva, Ph.D.

Anesthesiology 2020; 132:307–20

EDITOR'S PERSPECTIVE

What We Already Know about This Topic

- Both pressure-support and pressure-controlled ventilation may be used in patients with acute respiratory distress syndrome
- The importance of static and dynamic transpulmonary driving pressure during mechanical ventilation is not well understood

What This Article Tells Us That Is New

- In a rat model of mild lung injury caused by intratracheal endotoxin administration, animals received both pressure-support and pressure-controlled ventilation, and effects on driving pressures were measured, along with lung inflammation and diaphragm inflammation
- Pressure-support *versus* pressure-controlled ventilation was associated with higher dynamic (but not static) transpulmonary driving pressure, while markers of lung and diaphragm inflammation did not differ between ventilation modes

ABSTRACT

Background: Pressure-support ventilation may worsen lung damage due to increased dynamic transpulmonary driving pressure. The authors hypothesized that, at the same tidal volume (V_T) and dynamic transpulmonary driving pressure, pressure-support and pressure-controlled ventilation would yield comparable lung damage in mild lung injury.

Methods: Male Wistar rats received endotoxin intratracheally and, after 24 h, were ventilated in pressure-support mode. Rats were then randomized to 2 h of pressure-controlled ventilation with V_T, dynamic transpulmonary driving pressure, dynamic transpulmonary driving pressure, and inspiratory time similar to those of pressure-support ventilation. The primary outcome was the difference in dynamic transpulmonary driving pressure between pressure-support and pressure-controlled ventilation at similar V_T; secondary outcomes were lung and diaphragm damage.

Results: At V_T = 6 ml/kg, dynamic transpulmonary driving pressure was higher in pressure-support than pressure-controlled ventilation (12.0 ± 2.2 *vs.* 8.0 ± 1.8 cm H_2O), whereas static transpulmonary driving pressure did not differ (6.7 ± 0.6 *vs.* 7.0 ± 0.3 cm H_2O). Diffuse alveolar damage score and gene expression of markers associated with lung inflammation (interleukin-6), alveolar-stretch (amphiregulin), epithelial cell damage (club cell protein 16), and fibrogenesis (metalloproteinase-9 and type III procollagen), as well as diaphragm inflammation (tumor necrosis factor-α) and proteolysis (muscle RING-finger-1) were comparable between groups. At similar dynamic transpulmonary driving pressure, as well as dynamic transpulmonary driving pressure and inspiratory time, pressure-controlled ventilation increased V_T, static transpulmonary driving pressure, diffuse alveolar damage score, and gene expression of markers of lung inflammation, alveolar stretch, fibrogenesis, diaphragm inflammation, and proteolysis compared to pressure-support ventilation.

Conclusions: In the mild lung injury model use herein, at the same V_T, pressure-support compared to pressure-controlled ventilation did not affect biologic markers. However, pressure-support ventilation was associated with a major difference between static and dynamic transpulmonary driving pressure; when the same dynamic transpulmonary driving pressure and inspiratory time were used for pressure-controlled ventilation, greater lung and diaphragm injury occurred compared to pressure-support ventilation.

(ANESTHESIOLOGY 2020; 132:307–20)

Pressure-support ventilation has been recommended for use in mild acute respiratory distress syndrome (ARDS)[1] due to its potential beneficial effects on hemodynamics,[2] reduced need for sedation,[3] and diaphragm protection.[4,5] However, during pressure-support ventilation, ventilator-induced lung injury may occur due to several

This article is featured in "This Month in Anesthesiology," page 1A. Supplemental Digital Content is available for this article. Direct URL citations appear in the printed text and are available in both the HTML and PDF versions of this article. Links to the digital files are provided in the HTML text of this article on the Journal's Web site (www.anesthesiology.org). The protocol and results of this study have been presented in part at the American Thoracic Society scientific meeting on May 23, 2018 in San Diego, California, and were previously published as an abstract (American Journal of Respiratory and Critical Care Medicine 2018; 197:A7523).

Submitted for publication September 26, 2018. Accepted for publication October 17, 2019. Published online first on November 21, 2019. From the Laboratory of Pulmonary Investigation, Carlos Chagas Filho Biophysics Institute, Federal University of Rio de Janeiro, Rio de Janeiro, Brazil (E.F.P., R.S.S., M.A.A., L.A.M., G.A.P., J.D.A.M., A.C.F.C., M.V.S.F., P.R.M.R., P.L.S.); Department of Pathology, School of Medicine, University of São Paulo, São Paulo, Brazil (V.L.C.); Pulmonary Engineering Group, Department of Anesthesiology and Intensive Care Therapy, University Hospital Carl Gustav Carus, Dresden University of Technology, Dresden, Germany (M.G.D.A.); Department of Integrated Surgical and Diagnostic Sciences, University of Genoa, Genoa, Italy (P.P.); and Institute of Admission and Care of a Scientific Nature, San Martino Policlinico Hospital, Genoa, Italy (P.P.).

 Anesthesiology 2020; 132:307–20. DOI: 10.1097/ALN.0000000000003060

<zdoi;. DOI: 10.1097/ALN.0000000000003060>

factors: (1) increased spontaneous breathing effort and, thus, transpulmonary driving pressure[5] and tensile stress[6]; (2) patient–ventilator asynchrony[7]; (3) *pendelluft* and inhomogeneous stretch across the lungs[8]; and (4) alveolar edema, as negative pleural pressures can be transmitted to the alveoli, increasing capillary perfusion.[9]

To mitigate ventilator-induced lung injury during pressure-support ventilation, tidal volume (V_T) and transpulmonary driving pressure must be tightly controlled.[5] Different methods have been described to measure transpulmonary driving pressure during pressure-support ventilation.[10] However, the impact of static and dynamic transpulmonary driving pressure on lung damage has not been clearly elucidated.

To date, no study has evaluated whether static or dynamic transpulmonary driving pressure has any biologic impact on the lung in either pressure-support ventilation or pressure-controlled ventilation. We hypothesized that (1) at the same V_T, when combined with similar static transpulmonary driving pressure but higher dynamic transpulmonary driving pressure, pressure-support ventilation and pressure-controlled ventilation would be associated with similar lung damage; and (2) at the same dynamic transpulmonary driving pressure, when combined with higher V_T and static transpulmonary driving pressure, pressure-controlled ventilation would result in greater lung injury compared to pressure-support ventilation. For this purpose, mild lung injury was induced in rats by endotoxin instillation, and animals were ventilated in pressure-support mode. Once mean V_T and dynamic transpulmonary driving pressure values during pressure-support ventilation were known, animals were ventilated in pressure-controlled ventilation with either V_T or dynamic transpulmonary driving pressure obtained in the pressure-support ventilation group. Lung function and histology, as well as gene expression of markers associated with pulmonary inflammation, alveolar stretch, epithelial and endothelial cell damage, extracellular matrix organization, diaphragm inflammation, and proteolysis were analyzed.

Materials and Methods

Study Approval

This study was approved by the Ethics Committee of the Carlos Chagas Filho Institute of Biophysics (CEUA 105/16), Federal University of Rio de Janeiro, Rio de Janeiro, Brazil. All animals received humane care in compliance with the "Principles of Laboratory Animal Care" formulated by the National Society for Medical Research (Washington, DC) and the *Guide for the Care and Use of Laboratory Animals* prepared by the National Academy of Sciences, (Washington, DC). The current study followed the Animal Research: Reporting of *In Vivo* Experiments guidelines for reporting of animal research.[11] Animals were housed at a controlled temperature (23°C) and controlled light–dark cycle (12–12 h), with free access to water and food.

Animal Preparation and Experimental Protocol

In the early morning (8:00 AM), 52 male Wistar rats (mean weight 443 ± 93 g) were anesthetized by inhalation of isoflurane 1.5 to 2.0% (Isoforine; Cristália, Brazil) during spontaneous breathing and underwent intratracheal instillation of 200 μg *Escherichia coli* lipopolysaccharide (O55:B5, LPS Ultrapure; InvivoGen, France), suspended in 0.9% saline solution (total volume 200 μl), to induce mild lung injury at the pulmonary investigation laboratory of a large medical research institute.[12] Animals were then allowed to recover from anesthesia and observed for a period of 24 h. After 24 h, animals were premedicated intraperitoneally with 10 mg/kg diazepam (Compaz; Cristália, Brazil), followed by 100 mg/kg ketamine (Ketamin-S+; Cristália, Brazil) and 2 mg/kg midazolam (Dormicum; União Química, Brazil). After local anesthesia with 2% lidocaine (0.4 ml), a midline neck incision and tracheostomy were performed, and rats were intubated with a polyethylene tube (ID 1.8 mm). The tube was connected to an airway pressure transducer and a two-sidearm pneumotachograph (ID 2.7 mm, length 25.7 mm, internal volume 0.147 ml, airflow resistance 0.0057 cm $H_2O \cdot ml^{-1} \cdot s^{-1}$).[13]

An intravenous (iv) catheter (Jelco 24G; Becton, Dickinson and Company, USA) was inserted into the tail vein and anesthesia induced and maintained with midazolam (2 mg $\cdot$ kg^{-1} $\cdot$ h^{-1}) and ketamine (50 mg $\cdot$ kg^{-1} $\cdot$ h^{-1}). The adequacy of anesthesia was assessed by response to a nociceptive stimulus before surgery. Additionally, Ringer's lactate (B. Braun, Switzerland) was administered intravenously at a rate of 10 ml $\cdot$ kg^{-1} $\cdot$ h^{-1}; Gelafundin (B. Braun, Brazil) was intravenously administered in 0.5-ml boluses as necessary to maintain a mean arterial pressure (MAP) greater than 60 mmHg. A second catheter (18G; Arrow International, USA) was then placed in the right internal carotid artery for blood sampling and arterial blood gas analysis (ABL80 FLEX; Radiometer Medical, Denmark), as well as monitoring of MAP (Networked Multiparameter Veterinary Monitor LifeWindow 6000V; Digicare Animal Health, USA). A 30-cm-long water-filled catheter (PE-205; Becton, Dickinson and Company) with side holes at the tip, connected to a differential pressure transducer (UT-PL-400; SCIREQ, Canada), was used to measure the esophageal pressure. Briefly, the esophageal catheter was passed into the stomach and then slowly returned into the esophagus; its proper positioning was assessed using the "occlusion test." This method consists of comparing the variation between esophageal pressure and positive airway pressure (P_{aw}) during spontaneous inspiratory efforts made against a closed airway. When the changes in esophageal pressure and P_{aw} are comparable (difference of 5% and phase angle close to nil), this indicates that the changes in esophageal pressure provide a valid measure of changes in pleural pressure.[14] Heart rate, MAP, and rectal temperature were monitored continuously (Networked Multiparameter Veterinary Monitor LifeWindow 6000V; Digicare Animal Health).

Body temperature was maintained at 37.5 ± 1°C with a heating bed.

Eight of the 52 rats were subjected to *E. coli* lipopolysaccharide instillation, but not ventilated. This nonventilated group was used for molecular biology analysis. Initially, eight animals were mechanically ventilated in pressure-support ventilation mode (n = 8), in sequential order, using the following settings, in accordance with previous studies[12,15]: pressure support adjusted to V_T = 6 ml/kg, fraction of inspired oxygen = 0.4, and positive end-expiratory pressure (PEEP) = 3 cm H_2O. Flow trigger sensitivity was adjusted for adequate inspiratory effort, according to esophageal pressure decay.[16,17] The Servo-I switches from inspiration to expiration when the inspiratory flow has decayed to less than 25% of the peak inspiratory value. Therefore, the end inspiratory flow, although not necessarily nil, is always relatively low. Lung mechanics were assessed at the start of mechanical ventilation (INITIAL) and after 2 h (FINAL). Once mean V_T, dynamic transpulmonary driving pressure, and inspiratory time values during pressure-support ventilation were known, animals were randomly assigned to 2 h of mechanical ventilation in pressure-controlled ventilation with (1) V_T values similar to those obtained in the pressure-support ventilation group (n = 8); (2) dynamic transpulmonary driving pressure values similar to those obtained in the pressure-support ventilation group (n = 8); or (3) dynamic transpulmonary driving pressure and inspiratory time similar to those obtained in the pressure-support ventilation group (n = 8; fig. 1A). As pressure-controlled ventilation inherently requires neuromuscular blockade, animals in this group were paralyzed by intravenous administration of pancuronium bromide (1 mg/kg; Cristália, Brazil). To ensure comparable minute ventilation among groups, the respiratory

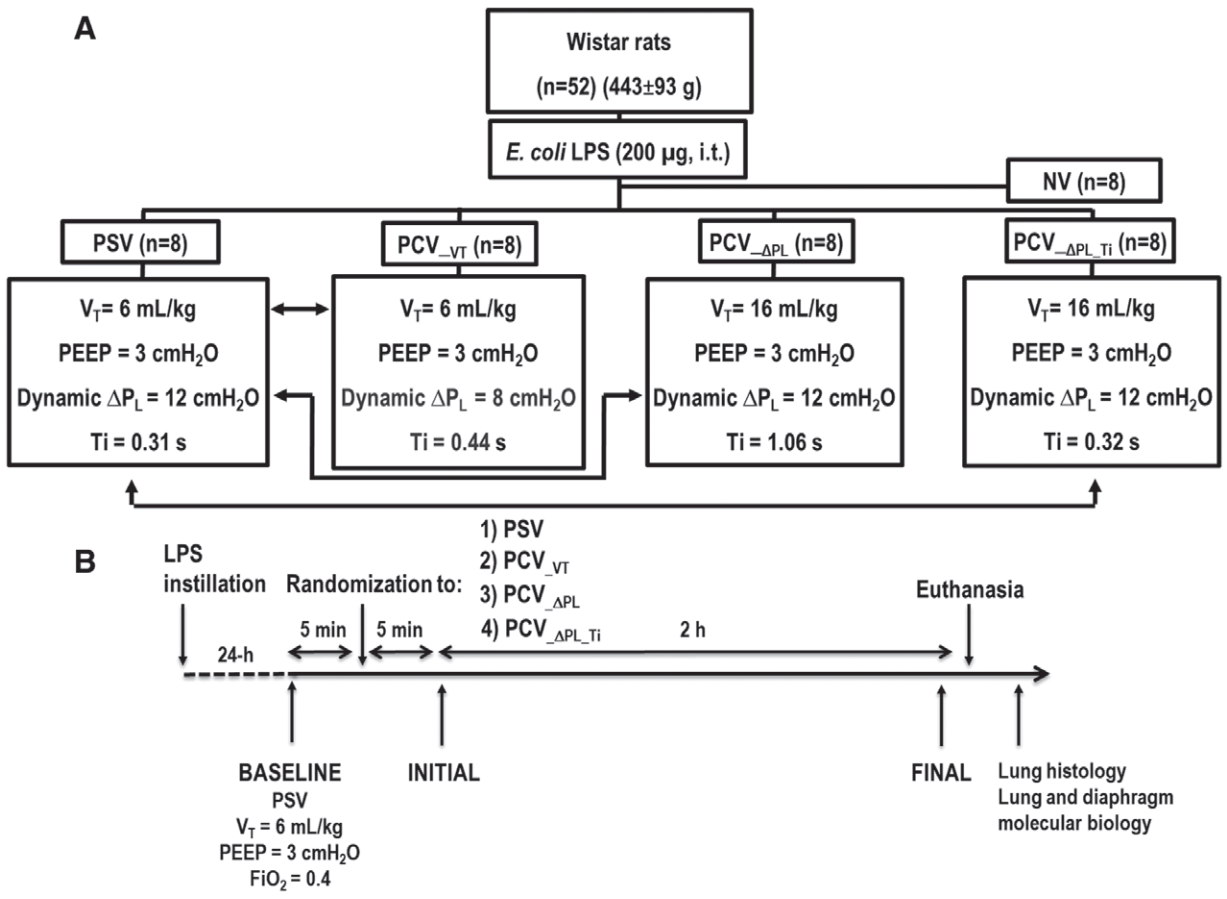

Fig. 1. Schematic flowchart of study design (*A*) and timeline representation of the experimental protocol (*B*). The total number of animals (n = 52) refers to 40 animals represented in the schematic flowchart with addition of 12 animals (4 animals per group) to calculate lung dynamic and static compliances. *E. coli* LPS, *Escherichia coli* lipopolysaccharide; FiO_2, fraction of inspired oxygen; i.t., intratracheally; NV, nonventilated; $PCV_{\Delta PL}$, pressure-controlled ventilation with dynamic transpulmonary driving pressure (ΔP_L) similar to that achieved by pressure-support ventilation; $PCV_{\Delta PL\_Ti}$, pressure-controlled ventilation with dynamic ΔP_L and inspiratory time (Ti) similar to that achieved by pressure-support ventilation; PCV_{VT}, pressure-controlled ventilation with the same tidal volume (V_T) of pressure-support ventilation; PEEP, positive end-expiratory pressure; PSV, pressure-support ventilation adjusted to V_T = 6 ml/kg.

rate was modified accordingly. *A priori*, we defined that, in order to achieve a dynamic transpulmonary driving pressure similar to those obtained during pressure-support ventilation, V_T would increase in pressure-controlled ventilation.[18] At FINAL, heparin was intravenously injected (1,000 U), and animals were euthanized by intravenous overdose of sodium thiopental (60 mg/kg; Cristália, Brazil). The trachea was clamped at PEEP = 3 cm H_2O, and the lungs were removed *en bloc* for histology and molecular biology analysis. The diaphragm was also removed at the end of the experiments (fig. 1B).

Data Acquisition and Lung Mechanics

Airflow, P_{aw}, and esophageal pressure were recorded continuously throughout the experiments by a computer running customer-made software written in LabVIEW (National Instruments, USA). V_T was calculated by digital integration of the airflow signal. All signals were amplified in a four-channel signal conditioner (SC-24; SCIREQ, Canada) and sampled at 200 Hz with a 12-bit analog-to-digital converter (National Instruments). Dynamic transpulmonary driving pressure (ΔP_L) was calculated at the end of inspiration (max) and expiration (min) as the difference between the delta P_{aw} (ΔP_{aw}) and delta esophageal pressure (ΔPes), according to the following equation 1[19]: $\Delta P_L = \Delta P_{aw} - \Delta Pes$

where and $\Delta Pes = Pes_{max} - Pes_{min}$.

For each selected breath, the time point of maximal decay in esophageal pressure guided the same time point of inspiratory P_{aw} (Supplemental Digital Content, fig. 1, http://links.lww.com/ALN/C105). Thus, we calculated the dynamic transpulmonary driving pressure from the airway (ΔP_{aw}) and esophageal (ΔPes) pressure swings, without inspiratory pauses. As mismatch between maximal esophageal pressure decay and the peak airway pressure in some respiratory cycles (less than 10%) has been observed elsewhere,[8] only the best-matched cycles between inspiratory airway pressure and maximal esophageal pressure nadir signals were used to calculate dynamic transpulmonary driving pressure. The other cycles in which esophageal pressure nadir and airway peak pressure did not coincide were not considered. The difference in dynamic transpulmonary driving pressure between the breaths included in the analysis and all breaths was less than 5%, which is within the variability range of dynamic transpulmonary driving pressure. Respiratory rate was calculated from esophageal pressure swings as the frequency per minute of each type of breathing cycle. In response to peer review, additional experiments were done in 12 animals (4 animals per group) to calculate lung dynamic (V_T/dynamic transpulmonary driving pressure) and static compliance [V_T/static transpulmonary driving pressure ([airway plateau pressure–PEEP] − [esophageal plateau pressure–end-expiratory esophageal pressure]). To calculate plateau pressure, the airways were occluded at end-inspiration. During inspiratory pauses (3 s), when airflow was zero, the possible role of different inspiratory time, resistive components, and pressure generated by inspiratory muscles could be ruled out in pressure-support and pressure-controlled ventilation modes. The inspiratory time, total breathing cycle time, and the ratio between them in each ventilator strategy were also calculated. Dynamic intrinsic PEEP was quantified according to the first signs of esophageal pressure decay (inspiratory effort) and the onset of inspiratory flow.[20] All mechanical data were computed offline by a routine written in MATLAB (Version R2007a; The Mathworks Inc., USA).

Histology

Diffuse Alveolar Damage

The left lung was fixed in 4% formaldehyde solution and embedded in paraffin. Sections (4 μm thick) were cut longitudinally from the central zone with a microtome and stained with hematoxylin–eosin for histologic analysis. Photomicrographs at magnifications of ×25, ×100, and ×400 were obtained from eight nonoverlapping fields of view per section under a light microscope (Olympus BX51; Olympus Latin America Inc., Brazil). Diffuse alveolar damage was quantified by an expert in lung pathology (V.L.C.) blinded to group assignment, using a weighted scoring system described elsewhere,[21] which takes into account interstitial edema, inflammatory infiltration, and ductal overdistension. The total diffuse alveolar damage score was the sum of these three features and thus ranged from 0 to 48.

Morphometric Analysis

Lung morphometric analysis was performed using an integrating eyepiece with a coherent system consisting of a grid with 100 points and 50 lines of known length coupled to the same light microscope described above. The volume fractions of the lung occupied by collapsed alveoli were determined by the point-counting technique at a magnification of ×200 across. Lung morphometry was quantified by two investigators (V.L.C. and A.C.F.C.) blinded to group assignment.

Quantification of Heterogeneous Airspace Enlargement

Airspace enlargement was assessed by measuring the mean linear intercept between alveolar walls at a magnification of ×400, as described elsewhere.[22] To characterize the heterogeneity of airspace enlargement, the central moment of the mean linear intercept (D_2 of mean linear intercept between alveolar walls) was computed from 20 airspace measurements,[23] according to equation 2:

$$D_2 = \mu \cdot \left(1 + \frac{\sigma^2}{\mu^2 + \sigma^2}\right) \cdot \left(2 + \sigma \cdot \frac{\gamma}{\mu}\right) \quad (2)$$

where μ is the mean, σ is the variance of airspace diameters, and γ is the skewness of the diameter distribution. After

D_2 calculation, the heterogeneity index was derived from D_2 and mean linear intercept between alveolar wall values by their ratio.[24] Quantification of heterogeneous airspace enlargement was performed by two investigators (V.L.C. and M.V.S.F.) blinded to group assignment.

Immunohistochemistry

To analyze the adherent junction protein E-cadherin, immunohistochemical procedures were performed on 4-μm-thick, paraffin-embedded lung sections using a mouse polyclonal antibody against E-cadherin (1:250, catalog No. 610181; BD Transduction Laboratories, USA). More detailed information can be found elsewhere.[12] Blinded analyses were carried out by two investigators (V.L.C. and A.C.F.C.).

Molecular Biology Analysis of Lung and Diaphragm Tissue

Quantitative real-time reverse transcription polymerase chain reaction was performed to measure biologic markers associated with inflammation (interleukin-6), alveolar stretch (amphiregulin), alveolar epithelial cell damage (club cell protein 16), endothelial cell damage (vascular cell adhesion molecule-1), fibrogenesis (metalloproteinase-9, type III procollagen) in lung tissue, as well as markers of inflammation (tumor necrosis factor-α) and muscle proteolysis (muscle RING-finger-1) in the diaphragm. The primer sequences are listed in Supplemental Digital Content, table 1, http://links.lww.com/ALN/C106. Central slices of right lung and diaphragm were cut, collected in cryotubes, quick-frozen by immersion in liquid nitrogen, and stored at −80°C. Total RNA was extracted from frozen tissues using the RNeasy Plus Mini Kit (Qiagen, Germany) for the lungs and RNeasy Fibrous Tissue Mini Kit (Qiagen) for the diaphragm, following the manufacturer's recommendations. The RNA concentration was measured by spectrophotometry in a Nanodrop ND-1000 system. First-strand complementary DNA was synthesized from total RNA using a Quantitec reverse transcription kit (Qiagen). Relative messenger RNA concentrations were measured with a SYBR green detection system using ABI 7500 real-time polymerase chain reaction (Applied Biosystems, USA). Samples were measured in triplicate. For each sample, the expression of each gene was normalized to that of the housekeeping gene *36B4* (acidic ribosomal phosphoprotein P0) and expressed as fold change relative to nonventilated, using the $2^{-\Delta\Delta Ct}$ method, where ΔCt = Ct (reference gene) − Ct (target gene). All analyses were performed by one of the authors (M.A.A.), who was blinded to group assignment.

Statistical Analysis

The sample size was judiciously calculated to minimize the use of animals. A sample of eight animals per group would provide the appropriate power ($1-\beta = 0.8$) to identify significant ($\alpha = 0.05$) differences in peak transpulmonary pressure between pressure-support and pressure-controlled ventilation,[15] taking into account an effect size $d = 1.62$, a two-sided test, and a sample size ratio of 1 (G*Power 3.1.9.2; University of Düsseldorf, Germany). The primary outcome was the difference in transpulmonary driving pressure between pressure-support and pressure-controlled ventilations, whereas the secondary outcomes were diffuse alveolar damage score, airspace heterogeneity, E-cadherin lung tissue expression, and expression of genes related to inflammation, alveolar stretch, epithelial and endothelial cell injuries, and fibrogenesis, as well as diaphragm inflammation and proteolysis. The Kolmogorov–Smirnov test with Lilliefors' correction was used to assess normality of data, while the Levene median test was used to evaluate the homogeneity of variances. To compare functional data at BASELINE, one-way between-subjects ANOVA followed by Tukey test was used. To compare functional parameters over time, a mixed linear model based on a random intercept for each animal followed by Bonferroni test was used. For diffuse alveolar damage, electron microscopy, airspace enlargement, immunohistochemistry, and molecular biology assays in lung and diaphragm tissue, the Mann–Whitney *U* test was done, according to Bonferroni correction for three comparisons (pressure-controlled ventilation at similar V_T observed in pressure support ventilation *vs.* pressure-support ventilation, pressure-controlled ventilation at similar transpulmonary driving pressure observed in pressure support ventilation *vs.* pressure-support ventilation, pressure-controlled ventilation at similar transpulmonary driving pressure and inspiratory time observed in pressure support ventilation *vs.* pressure-support ventilation; $P < 0.0167$). Spearman correlation and Bland–Altman analysis of dynamic transpulmonary driving pressure calculation were done as described by Bellani *et al.*[19] and Yoshida *et al.*[25] Parametric data are expressed as mean ± SD, and nonparametric data as median (interquartile range). Outliers were not removed. The mixed linear models were run in IBM SPSS Statistics for Windows, Version 19.0 (IBM Corp., USA). All other tests were performed in GraphPad Prism v6.07 (GraphPad Software, USA). Significance was established at $P < 0.05$.

Results

The survival rate was 100% in all groups; thus, there were no missing data. At BASELINE, functional data did not differ among groups (Supplemental Digital Content, table 2, http://links.lww.com/ALN/C107; n = 8 per group). At FINAL, no significant differences among groups were observed in the volume of fluids required to keep MAP 60 mmHg or greater (Supplemental Digital Content, table 3, http://links.lww.com/ALN/C108; n = 8 per group).

Our methods for dynamic transpulmonary driving pressure calculation showed a significant association ($r = 0.68$; $P < 0.001$) and good agreement (bias = –0.17; 95% CI, –1.8 to 1.4) with methods previously used in the literature (Supplemental Digital Content, fig. 2, http://links.lww.com/ALN/C109).

The cycling-off value during pressure-support ventilation ranged from 4.5 to 4.8 ml/s. At similar V_T (approximately 6 ml/kg), dynamic transpulmonary driving pressure was higher while static transpulmonary driving pressure was similar in pressure-support ventilation compared to pressure-controlled ventilation at similar V_T observed in pressure support ventilation (table 1, n = 8 per group). No major differences were observed in inspiratory time, the ratio between inspiratory time and total breathing cycle time, and dynamic intrinsic PEEP between pressure-support ventilation and pressure-controlled ventilation at similar V_T observed in pressure support ventilation animals (table 1, n = 8 per group). Lung dynamic compliance was higher in pressure-controlled ventilation at similar V_T observed in pressure support ventilation animals than pressure-support ventilation animals, while lung static compliance did not differ (Supplemental Digital Content, table 4, http://links.lww.com/ALN/C110; n = 4 per group). No major differences were observed in oxygenation (Supplemental Digital Content, table 3, http://links.lww.com/ALN/C108; n = 8 per group), diffuse alveolar damage score (table 2), or E-cadherin expression (Supplemental Digital Content, fig. 3, http://links.lww.com/ALN/C111; n = 8 per group) in lung tissue between pressure-support ventilation and pressure-controlled ventilation at similar V_T observed in pressure support ventilation animals. The heterogeneity index and alveolar collapse (fig. 2, n = 8 per group) were lower in pressure-support ventilation and pressure-controlled ventilation at similar V_T observed in pressure support ventilation animals, without significant differences in gene expression of interleukin-6, amphiregulin, club cell protein 16, vascular cell adhesion molecule-1, metalloproteinase-9, or type III procollagen in lung tissue (fig. 3, n = 8 per group), nor of tumor necrosis factor-α and muscle RING-finger-1 in the diaphragm (fig. 4, n = 8 per group).

At similar dynamic transpulmonary driving pressure, compared to pressure-support ventilation, both pressure-controlled ventilation at similar transpulmonary driving pressure observed in pressure support ventilation and pressure-controlled ventilation at similar transpulmonary driving pressure and inspiratory time observed in pressure support ventilation resulted in higher V_T, total breathing cycle time, and static transpulmonary driving pressure (table 1, n = 8 per group). In addition, tissue expression of E-cadherin was lower (Supplemental Digital Content, fig. 3, http://links.lww.com/ALN/C111; n = 8 per group), while diffuse alveolar damage score (table 2, n = 8 per group) and heterogeneity index were higher and alveolar collapse was reduced in both pressure-controlled ventilation at similar transpulmonary driving pressure observed in pressure support ventilation and pressure-controlled ventilation at similar transpulmonary driving pressure and inspiratory time observed in pressure support ventilation compared to pressure-support ventilation animals (fig. 2, n = 8 per group). Gene expressions of interleukin-6, amphiregulin, metalloproteinase-9, and type III procollagen in lung tissue were higher in pressure-controlled ventilation at similar transpulmonary driving pressure observed in pressure support ventilation compared to the pressure-support ventilation group (fig. 3, n = 8 per group). Club cell protein 16 and vascular cell adhesion molecule-1 gene expressions were higher in pressure-controlled ventilation at similar transpulmonary driving pressure and inspiratory time observed in pressure support ventilation and pressure-controlled ventilation at similar transpulmonary driving pressure observed in pressure support ventilation compared to pressure-support ventilation, respectively. In addition, tumor necrosis factor-α and muscle RING-finger-1 messenger RNA expressions in the diaphragm were higher in pressure-controlled ventilation at similar transpulmonary driving pressure observed in pressure support ventilation and pressure-controlled ventilation at similar transpulmonary driving pressure and inspiratory time observed in pressure support ventilation than pressure-support ventilation animals (fig. 4, n = 8 per group).

Discussion

In the rat model of mild lung injury used herein, we found that, at the same protective V_T (6 ml/kg), pressure-support ventilation resulted in higher dynamic transpulmonary driving pressure, similar static transpulmonary driving pressure, and lower airspace heterogeneity than pressure-controlled ventilation, but with no significant differences in diffuse alveolar damage score, E-cadherin protein content, biologic markers associated with lung inflammation (interleukin-6), alveolar stretch (amphiregulin), fibrogenesis (metalloproteinase-9 and type III procollagen), alveolar epithelial and endothelial cell damage, or markers of diaphragm inflammation (tumor necrosis factor-α) and proteolysis (muscle RING-finger-1). At the same dynamic transpulmonary driving pressure, with and without adjusted inspiratory time, pressure-controlled compared to pressure-support ventilation resulted in higher V_T and static transpulmonary driving pressure with increased diffuse alveolar damage score and airspace heterogeneity, reduced E-cadherin expression in lung tissue, and increased gene expression of interleukin-6, amphiregulin, metalloproteinase-9, and type III procollagen in lung tissue, as well as tumor necrosis factor-α and muscle RING-finger-1 in the diaphragm.

Our results suggest that static transpulmonary driving pressure, rather than dynamic transpulmonary driving pressure, is the main determinant of lung and diaphragm injury during pressure-support ventilation. These data are an important step forward to determine the best method to calculate static and dynamic transpulmonary driving pressure, as well as to evaluate their relevance to optimization of ventilator settings.

We chose to use a model of mild lung injury induced by intratracheal instillation of *E. coli* lipopolysaccharide because it reproduces several features of mild human ARDS.[26] Changes in lung histology associated with increased neutrophil infiltration were observed, as well as oxygenation impairment. Accordingly, this model mimics the conditions in which pressure-support ventilation has been recommended for clinical use in ARDS.[27] In the current study, V_T as well as dynamic and static transpulmonary driving

Table 1. Respiratory Variables during Mechanical Ventilation

	Groups	INITIAL	FINAL	Time Effect	Group Effect	Interaction
V_T (ml/kg)				$P = 0.553$	$P < 0.0001$	—
	PSV	6.0 ± 0.4	5.5 ± 0.7			
	PCV_{-VT}	6.4 ± 0.8	6.6 ± 0.7			
	$PCV_{-\Delta PL}$	16.8± 3.3	15.9 ± 3.1			
	$PCV_{-\Delta PL\_Ti}$	15.0 ± 4.3	15.5 ± 2.9			
RR (breaths per min)				$P = 0.949$	$P < 0.0001$	—
	PSV	60 ± 9	70 ± 17			
	PCV_{-VT}	56 ± 10	51 ± 6			
	$PCV_{-\Delta PL}$	19 ± 5	22 ± 5			
	$PCV_{-\Delta PL\_Ti}$	33 ± 4	39 ± 13			
Ti (s)				$P = 0.083$	$P < 0.001$	—
	PSV	0.36 ± 0.08	0.31 ± 0.08			
	PCV_{-VT}	0.44 ± 0.05	0.39 ± 0.08			
	$PCV_{-\Delta PL}$	1.06 ± 0.17	1.02 ± 0.16			
	$PCV_{-\Delta PL\_Ti}$	0.36 ± 0.04	0.32 ± 0.04			
Ttot (s)				$P = 0.369$	$P < 0.001$	—
	PSV	0.91 ± 0.17	0.81 ± 0.21			
	PCV_{-VT}	1.21 ± 0.11	1.36 ± 0.45			
	$PCV_{-\Delta PL}$	3.14 ± 0.54	2.93 ± 0.45			
	$PCV_{-\Delta PL\_Ti}$	1.83 ± 0.21	1.67 ± 0.43			
Ti/Ttot (s)				$P = 0.480$	$P < 0.001$	—
	PSV	0.39 ± 0.08	0.38 ± 0.08			
	PCV_{-VT}	0.36 ± 0.03	0.39 ± 0.09			
	$PCV_{-\Delta PL}$	0.33 ± 0.01	0.34 ± 0.03			
	$PCV_{-\Delta PL\_Ti}$	0.19 ± 0.02	0.21 ± 0.07			
Airflow (ml/s)				$P = 0.960$	$P = 0.001$	—
	PSV	19.0 ± 3.2	17.7 ± 2.8			
	PCV_{-VT}	20.0 ± 1.7	21.9 ± 4.7			
	$PCV_{-\Delta PL}$	25.6 ± 4.4	23.3 ± 5.0			
	$PCV_{-\Delta PL\_Ti}$	27.3 ± 11.3	28.4 ± 5.7			
V'_E (ml/min)				$P = 0.932$	$P = 0.144$	—
	PSV	203 ± 38	179 ± 31			
	PCV_{-VT}	158 ± 14	165 ± 18			
	$PCV_{-\Delta PL}$	137 ± 28	132 ± 21			
	$PCV_{-\Delta PL\_Ti}$	142 ± 61	154 ± 49			
Dynamic ΔP_L ($cm H_2O$)				$P = 0.740$	$P < 0.0001$	—
	PSV	12.9 ± 0.9	12.0 ± 2.2			
	PCV_{-VT}	7.8 ± 1.3	8.0 ± 1.8			
	$PCV_{-\Delta PL}$	12.5 ± 1.0	12.8 ± 0.6			
	$PCV_{-\Delta PL\_Ti}$	12.7 ± 0.4	12.0 ± 0.8			
Static ΔP_L ($cm H_2O$)				$P = 0.027$	$P < 0.0001$	$P = 0.0007$
	PSV	7.2 ± 0.4	6.7 ± 0.6			
	PCV_{-VT}	6.8 ± 0.2	7.0 ± 0.3			
	$PCV_{-\Delta PL}$	11.8 ± 0.2*	12.1 ± 0.3*			
	$PCV_{-\Delta PL\_Ti}$	11.8 ± 0.5*	10.8 ± 1.1*			
PEEPi,dyn ($cm H_2O$)				$P = 0.497$	$P = 0.109$	—
	PSV	0.6 ± 0.2	0.7 ± 0.3			
	PCV_{-VT}	0.6 ± 0.3	0.7 ± 0.3			
	$PCV_{-\Delta PL}$	0.8 ± 0.3	0.6 ± 0.5			
	$PCV_{-\Delta PL\_Ti}$	0.3 ± 0.4	0.2 ± 0.4			

Respiratory variables obtained at INITIAL and FINAL. Values are means ± SD of eight animals in each group. Comparisons were done using a mixed linear model followed by Bonferroni multiple comparisons ($P < 0.05$).

*, *vs.* PSV.

Dynamic ΔP_L, dynamic transpulmonary driving pressure; PCV_{VT}, pressure-controlled ventilation with the same V_T of pressure-support ventilation; $PCV_{\Delta PL}$, pressure-controlled ventilation with dynamic ΔP_L similar to that achieved by pressure-support ventilation; $PCV_{\Delta PL\_Ti}$, pressure-controlled ventilation with dynamic ΔP_L and inspiratory time (Ti) similar to that achieved by pressure-support ventilation; PEEPi,dyn, dynamic intrinsic positive end-expiratory pressure; PSV, pressure-support ventilation adjusted to tidal volume (V_T) = 6 ml/kg; RR, respiratory rate; static ΔP_L, static transpulmonary driving pressure; Ti/Ttot, respiratory time fraction; Ttot, total breathing cycle time; V'_E, minute ventilation.

pressure[19] were calculated in pressure-support mode and then compared with pressure-controlled ventilation. During pressure-support ventilation, transpulmonary pressure is determined by increased airway pressure and decreased pleural pressure, leading to tensile stress,[28] whereas during pressure-controlled ventilation, transpulmonary pressure is

Table 2. Cumulative Diffuse Alveolar Damage

	PSV	$PCV_{\_VT}$	$PCV_{\_\Delta PL}$	$PCV_{\_\Delta PL\_Ti}$
Interstitial edema (0–16)	1 (1–2)	2 (2–2.5)	4 (4–5)*	4 (4–6)*
Inflammatory infiltration (0–16)	4 (4–5)	5 (2–6.5)	9 (9–14)*	9 (7.5–12)*
Ductal overdistension (0–16)	2 (1–2)	2 (1.5–3)	12 (7.5–12)*	12 (9–13)*
Cumulative DAD (0–48)	7 (6–9)	10 (4.5–12)	27 (20.5–30)*	25 (23.5–28)*

Cumulative diffuse alveolar damage (DAD) score representing injury from interstitial edema, inflammatory infiltration, and ductal overdistension. Values are given as median (interquartile range) of eight animals in each group. Mann–Whitney *U* test with Bonferroni correction for three comparisons ($P < 0.0167$, $PCV_{\_VT}$ *vs.* PSV, $PCV_{\_\Delta PL}$ *vs.* PSV, and $PCV_{\_\Delta PL\_Ti}$ *vs.* PSV).

*, *vs.* PSV.

$PCV_{\_VT}$, pressure-controlled ventilation with the same V_T of pressure-support ventilation; $PCV_{\_\Delta PL}$, pressure-controlled ventilation with dynamic ΔP_L similar to that achieved by pressure-support ventilation; $PCV_{\_\Delta PL\_Ti}$, pressure-controlled ventilation with dynamic ΔP_L and inspiratory time (Ti) similar to that achieved by pressure-support ventilation; PSV, pressure-support ventilation adjusted to tidal volume (V_T) = 6 ml/kg.

achieved by a positive increase in airway and pleural pressures, leading to compressive stress.[19] Several studies have applied negative pressure to the thorax or abdomen in an attempt to mimic this decrease in intrapleural pressure and determine how such strategies compare with positive-pressure ventilation when either V_T or dynamic transpulmonary driving pressure are kept constant.[29–32] However, extrapolation of results from negative-pressure ventilation to settings where spontaneous breathing activity occurs may be inappropriate. Moreover, negative-pressure ventilation uses either continuous[29,30] or transient pressure,[31] both of which differ importantly from the more complex effects of respiratory muscle activity on intrapleural pressure.[5] Therefore, an important strength of the current study is the use of a ventilation strategy commonly employed in the clinical setting,[33] while isolating the impact of pressure-support ventilation *versus* pressure-controlled ventilation at the same V_T or dynamic transpulmonary driving pressure and static transpulmonary driving pressure, with and without adjusted inspiratory time, not only on lung mechanics and morphology, but also on biomarkers associated with inflammation, epithelial and endothelial cell damage, alveolar stretch, and extracellular matrix injury. In the current study, we compared pressure-controlled *versus* pressure-support ventilation in the following conditions: (1) comparable static transpulmonary driving pressure and V_T with different dynamic transpulmonary driving pressure; (2) comparable dynamic transpulmonary driving pressure with different static transpulmonary driving pressure and V_T; and (3) comparable inspiratory time and dynamic transpulmonary driving pressure with different static transpulmonary driving pressure and V_T. After performing inspiratory airway occlusions at a zero-airflow condition, we were able to measure static transpulmonary driving pressure (Supplemental Digital Content, fig. 4, http://links.lww.com/ALN/C112), which was similar between the pressure-support ventilation and pressure-controlled ventilation at similar V_T observed in pressure support ventilation groups. At similar V_T, pressure-support ventilation resulted in comparable static transpulmonary driving pressure and higher dynamic transpulmonary driving pressure, less alveolar collapse, and less airspace heterogeneity than pressure-controlled ventilation. In a previous study also conducted in mild lung injury,[25] pressure-support ventilation improved lung morphology parameters, but dynamic transpulmonary driving pressure did not differ between pressure-controlled ventilation and pressure-support ventilation. The balance between increased dynamic transpulmonary driving pressure and more homogeneous distribution of regional pleural pressure during pressure-support ventilation may contribute to the absence of changes in biomarkers of interest.

On the other hand, at similar dynamic transpulmonary driving pressure, V_T, static transpulmonary driving pressure, airspace heterogeneity, and diffuse alveolar damage score increased, whereas alveolar collapse decreased in pressure-control ventilation compared to pressure-support ventilation. These histologic changes may have contributed to increased gene expression of markers associated with lung inflammation, fibrogenesis, alveolar stretch, and alveolar epithelial cell damage. Moreover, alveolar integrity was reduced, as reflected by lower E-cadherin expression.[12] In fact, it has been shown that increased V_T is a key mechanism of ventilator-induced lung injury,[34] and may be especially injurious during nonhomogeneous distribution of strain across the lungs.[35] We cannot rule out the possibility that increased damage to the lung parenchyma during pressure-controlled ventilation at similar transpulmonary driving pressure observed in pressure support ventilation resulted from compressive stress, which has been shown to be more injurious than tensile stress, as it occurs during pressure-support ventilation.[36] Also, at the same dynamic transpulmonary driving pressure, lower intrapleural pressures during pressure-support ventilation as compared to pressure-controlled ventilation may have resulted in improved lymphatic dynamics and fluid clearance from lung tissue.[37] Pressure-controlled ventilation at similar transpulmonary driving pressure observed in pressure support ventilation and pressure-controlled ventilation at similar transpulmonary driving pressure and inspiratory time observed in pressure support ventilation, compared to pressure-support ventilation, resulted in increased gene expression of markers associated with diaphragm inflammation and proteolysis.

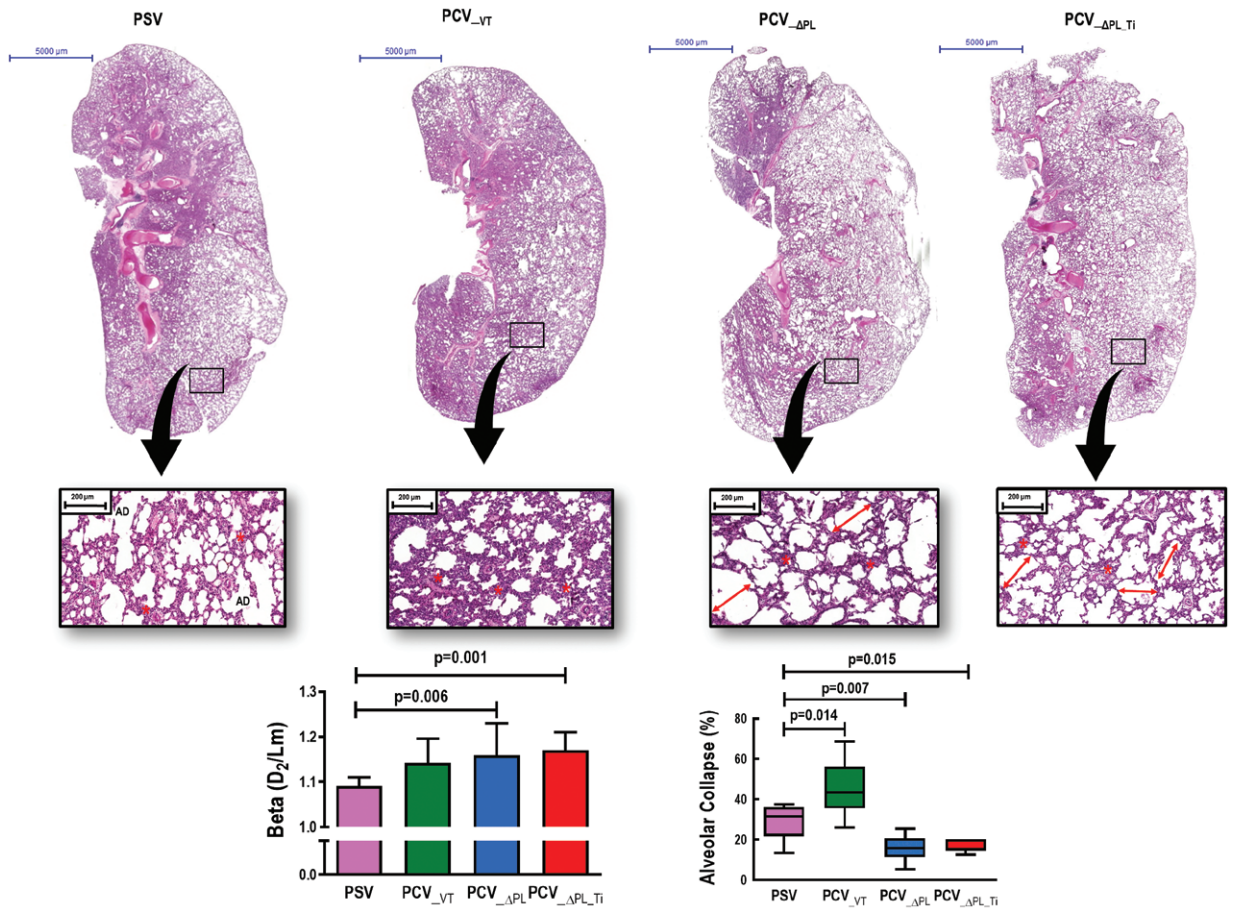

Fig. 2. Lung morphometry in mechanically ventilated animals. *Bars* represent mean ± SD of eight animals in each group. *Asterisks* show alveolar collapse. *Arrows* indicate alveolar overdistension. Alveolar collapse indicates the fractional area of lung occupied by collapsed alveoli. *Box plots* represent the median and interquartile range of eight animals in each group. Mann–Whitney *U* test with Bonferroni correction for multiple comparisons ($P < 0.0167$, $PCV_{\_VT}$ *vs.* PSV, $PCV_{\_\Delta PL}$ *vs.* PSV, and $PCV_{\_\Delta PL\_Ti}$ *vs.* PSV). AD, alveolar duct; β, heterogeneity index; D_2/Lm, central moment of the mean linear intercept (D_2 of mean linear intercept between alveolar walls); $PCV_{\_\Delta PL}$, pressure-controlled ventilation with dynamic ΔP_L similar to that achieved by pressure-support ventilation; $PCV_{\_\Delta PL\_Ti}$, pressure-controlled ventilation with dynamic ΔP_L and inspiratory time ($\bar{T}i$) similar to that achieved by pressure-support ventilation; $PCV_{\_VT}$, pressure-controlled ventilation with the same V_T of pressure-support ventilation; PSV, pressure-support ventilation adjusted to $V_T = 6$ ml/kg; V_T, tidal volume.

Accordingly, in healthy rats, pressure-support ventilation has been shown to protect against proteolysis compared to pressure-controlled ventilation,[38] thus minimizing diaphragm injury. During pressure-controlled ventilation at similar transpulmonary driving pressure observed in pressure support ventilation and pressure-controlled ventilation at similar transpulmonary driving pressure and inspiratory time observed in pressure support ventilation, the increase in V_T may change the shape of the diaphragm and promote muscle overstretch, leading to inflammation.[39]

Comparison between dynamic and static transpulmonary driving pressure measurements in pressure-support ventilation and pressure-controlled ventilation is challenging, since intraalveolar pressure would differ at different inspiratory times. In fact, longer inspiratory times would result in higher dynamic transpulmonary driving pressure and increased lung injury.[40] We found that pressure-controlled ventilation at similar dynamic transpulmonary driving pressure and inspiratory time induced greater lung injury than pressure-support ventilation, thus suggesting that parameters other than intraalveolar pressure (*e.g.*, inspiratory airflow) may play a relevant role in determining lung damage.[41,42]

Possible Clinical Implications

Our results suggest that, in mild ARDS, pressure-support ventilation was as protective as pressure-controlled ventilation despite higher dynamic transpulmonary driving pressure when a protective V_T and static transpulmonary driving pressure were used; and, at comparable dynamic transpulmonary driving pressure,

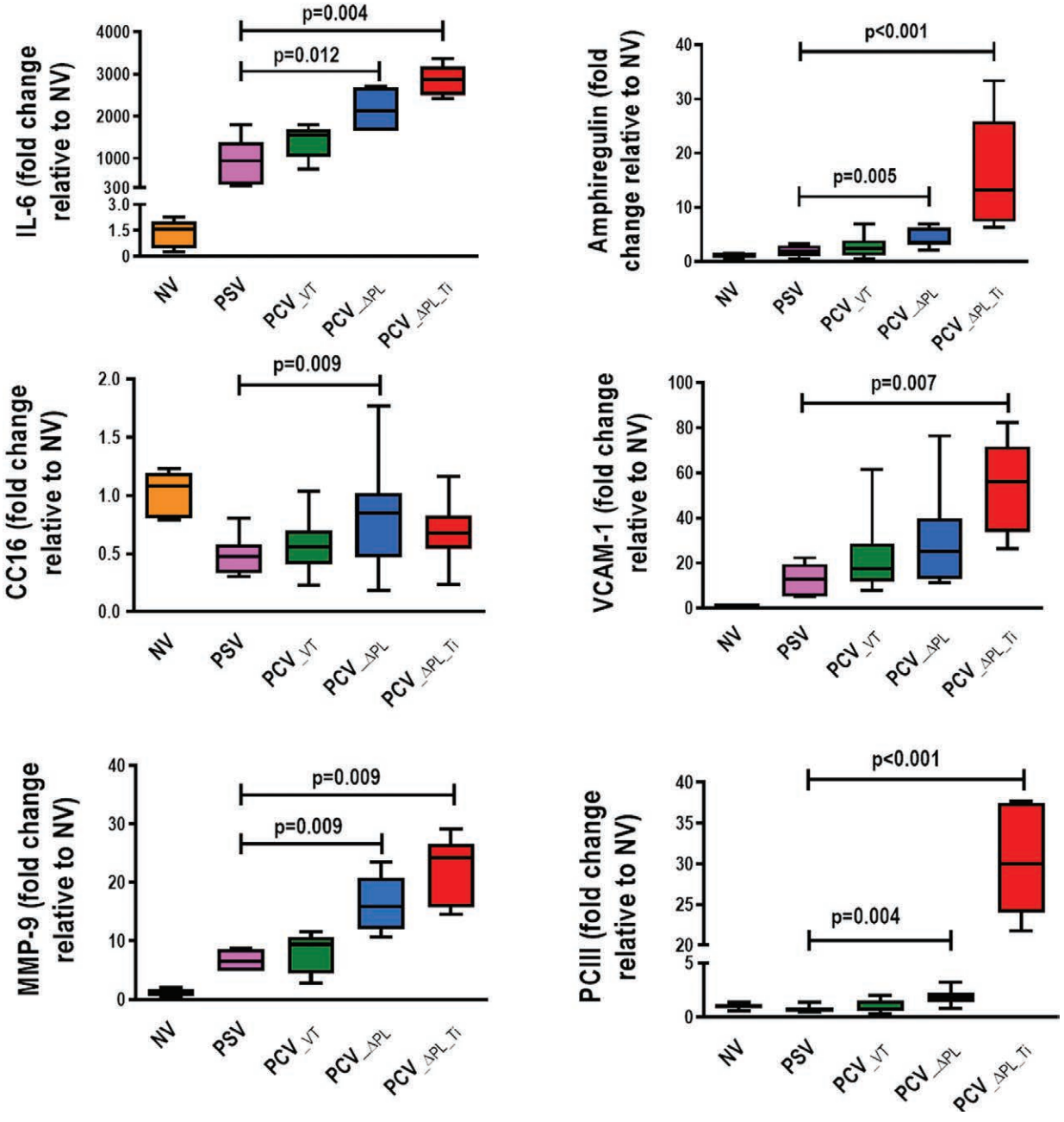

Fig. 3. Quantitative real-time polymerase chain reaction analysis of biologic markers of inflammation (interleukin [IL]-6), alveolar stretch (amphiregulin), epithelial (club cell protein [CC]16) and endothelial (vascular cell adhesion molecule [VCAM]-1) cell damage, and fibrogenesis (metalloproteinase [MMP]-9 and type III procollagen [PCIII]). Data are presented as a *box plot*. *Lines* denote the median, and *boxes* delimit the 25th and 75th percentiles of eight animals per group. Relative gene expression was calculated as a ratio of the average gene expression values compared with the reference gene *36B4* and expressed as fold change relative to nonventilated (NV). Mann–Whitney *U* test with Bonferroni correction for multiple comparisons ($P < 0.0167$, PCV_{VT} *vs.* PSV, $PCV_{\Delta PL}$ *vs.* PSV, and $PCV_{\Delta PL\_Ti}$ *vs.* PSV). $PCV_{\Delta PL}$, pressure-controlled ventilation with dynamic ΔP_L similar to that achieved by pressure-support ventilation; $PCV_{\Delta PL\_Ti}$, pressure-controlled ventilation with dynamic ΔP_L and inspiratory time (Ti) similar to that achieved by pressure-support ventilation; PCV_{VT}, pressure-controlled ventilation with the same V_T of pressure-support ventilation; PSV, pressure-support ventilation adjusted to $V_T = 6$ ml/kg; V_T, tidal volume.

with and without adjusted inspiratory time, pressure-controlled ventilation induced greater lung and diaphragm damage, likely due to increased V_T and static transpulmonary driving pressure. Therefore, the impact of dynamic and static transpulmonary driving pressure on ventilator-induced lung injury will differ considerably depending on whether mechanical stress is

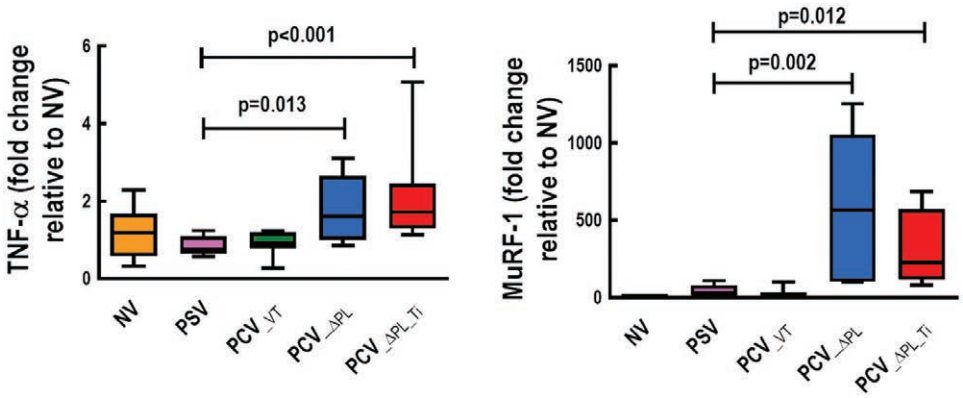

Fig. 4. Quantitative real-time polymerase chain reaction analysis of biologic markers associated with inflammation (tumor necrosis factor [TNF]-α) and muscle proteolysis (muscle RING-finger-1 [MuRF1]). Data are presented as a *box plot*. *Lines* denote the median, and *boxes* delimit the 25th and 75th percentiles of eight animals per group. Relative gene expression was calculated as a ratio of the average gene expression values compared with the reference gene *36B4* and expressed as fold change relative to nonventilated (NV). Mann–Whitney *U* test with Bonferroni correction for multiple comparisons ($P < 0.0167$, $PCV_{\_VT}$ *vs.* PSV, $PCV_{\_\Delta PL}$ *vs.* PSV, and $PCV_{\_\Delta PL\_Ti}$ *vs.* PSV). $PCV_{\_\Delta PL}$, pressure-controlled ventilation with dynamic ΔP_L similar to that achieved by pressure-support ventilation; $PCV_{\_\Delta PL\_Ti}$, pressure-controlled ventilation with dynamic ΔP_L and inspiratory time (Ti) similar to that achieved by pressure-support ventilation; $PCV_{\_VT}$, pressure-controlled ventilation with the same V_T of pressure-support ventilation; PSV, pressure-support ventilation adjusted to $V_T = 6$ ml/kg; V_T, tidal volume.

generated by tensile stress, as in pressure-support ventilation, or compressive stress, as in pressure-controlled ventilation.

Limitations

This study has some limitations. First, the rat model used does not reproduce all features of human ARDS. Second, our results may not apply to moderate or severe ARDS in experimental or clinical settings. Third, only male animals were used, both because they grow faster than female rats and to avoid any influence of hormonal fluctuation as a confounder on inflammatory parameters. Fourth, animals included in the pressure-support ventilation group did not undergo randomization; this was a necessity of our design, to ensure matching of dynamic transpulmonary driving pressure between the pressure-support ventilation and pressure-controlled ventilation at similar transpulmonary driving pressure observed in pressure support ventilation groups. Possible bias was reduced by using the same source of lipopolysaccharide, performing experiments in the same rat strain, and randomly assigning remaining animals to the pressure-controlled ventilation at similar transpulmonary driving pressure observed in pressure support ventilation, pressure-controlled ventilation at similar transpulmonary driving pressure and inspiratory time observed in pressure support ventilation, or pressure-controlled ventilation at similar Vt observed in pressure support ventilation groups. Fifth, esophageal manometry may be more representative of the dependent area during mechanical ventilation, especially in large animals,[43] and could be important to compute regional transpulmonary pressure. Notably, rats have a reduced vertical gradient compared to large animals, which may minimize the effects of regional transpulmonary pressure. Nevertheless, matching dynamic transpulmonary driving pressure in spontaneous *versus* controlled ventilation could be done in large animals by using pleural sensors or electric impedance tomography. Sixth, since the ventilation period was limited to 2 h, we were unable to detect protein content of biomarkers, except of E-cadherin, which is constitutively present in the alveolar epithelium. Seventh, the PEEP level was fixed at 3 cm H_2O, and we cannot rule out the possibility that higher or lower PEEP values might yield different results. Eighth, only the best-matched cycles between inspiratory airway and maximal esophageal pressures were analyzed to calculate transpulmonary driving pressure. Finally, during pressure-support ventilation, the alveolar pressure is equal the P_{aw} when flow is zero, and respiratory muscles are relaxed. The higher the activity of the respiratory muscles, the greater the difference between P_{aw} and alveolar pressure. In this case, the dynamic transpulmonary pressure may overestimate the transpulmonary pressure across the alveoli, not including the resistive pressure drop. In our study, the activity of the respiratory muscles at the end of inspiration was evaluated. We found that after airway occlusion, a relaxation of the respiratory muscles at end-inspiration was reached during pressure-support ventilation. Thus, P_{aw} may overestimate alveolar pressure only during a short period of the inspiratory phase. Since the maximum esophageal pressure swings during inspiration were approximately 2.6 cm H_2O and included the resistive components (1.2 to 1.5 cm H_2O), the overestimation of dynamic transpulmonary pressure during pressure-support ventilation was within a range of 1.2 to 0.9 cm H_2O, equivalent to approximately 10% of the total dynamic transpulmonary driving pressure. Therefore,

since V_T setting in pressure-controlled ventilation at similar transpulmonary driving pressure observed in pressure support ventilation is within the variability of the animals, our results may be not affected by this minor difference between the computation of dynamic transpulmonary pressure and V_T variation measured during pressure-support ventilation and pressure-controlled ventilation.

Conclusions

In the rat model of mild lung injury used herein, pressure-support ventilation did not affect biologic markers as compared to pressure-controlled ventilation at the same protective V_T. However, pressure-support ventilation resulted in a major difference between static and dynamic transpulmonary driving pressure, and when the same dynamic transpulmonary driving pressure, with and without adjusted inspiratory time, was used for pressure-controlled ventilation, it resulted in greater lung and diaphragm injury compared to pressure-support ventilation. Our data demonstrate the relevance of differences between static and dynamic transpulmonary driving pressure measurements for optimization of ventilator settings during pressure-controlled and pressure-support ventilation.

Acknowledgments

The authors express their gratitude to Andre Benedito da Silva, B.Sc., for animal care, Arlete Fernandes, B.Sc., for her help with microscopy, Maira Lima, B.Sc., for her help during the experiments (all from the Laboratory of Pulmonary Investigation, Institute of Biophysics Carlos Chagas Filho, Federal University of Rio de Janeiro, Rio de Janeiro, Brazil); Moira Elizabeth Schottler and Filippe Vasconcellos for their assistance in editing the manuscript; and Ronir Raggio Luiz (Institute of Studies in Collective Health, Federal University of Rio de Janeiro, Rio de Janeiro, Brazil) for his help with statistics.

Research Support

This study is supported by the Brazilian Council for Scientific and Technological Development, the Rio de Janeiro State Research Foundation (Rio de Janeiro, Brazil), the São Paulo State Research Foundation (São Paulo, Brazil), the National Institute of Science and Technology for Regenerative Medicine (Federal District, Brasilia, Brazil), and the Coordination for the Improvement of Higher Education Personnel (Federal District, Brasilia, Brazil).

Competing Interests

The authors declare no competing interests.

Correspondence

Address correspondence to Dr. Silva: Laboratory of Pulmonary Investigation, Carlos Chagas Filho Biophysics Institute, Federal University of Rio de Janeiro, Centro de Ciências da Saúde, Avenida Carlos Chagas Filho, 373, Bloco G-014, Ilha do Fundão, Rio de Janeiro, RJ 21941-902, Brazil. pedro.leme@gmail.com. Information on purchasing reprints may be found at www.anesthesiology.org or on the masthead page at the beginning of this issue. ANESTHESIOLOGY's articles are made freely accessible to all readers, for personal use only, 6 months from the cover date of the issue.

References

1. Bellani G, Laffey JG, Pham T, Fan E, Brochard L, Esteban A, Gattinoni L, van Haren F, Larsson A, McAuley DF, Ranieri M, Rubenfeld G, Thompson BT, Wrigge H, Slutsky AS, Pesenti A; LUNG SAFE Investigators; ESICM Trials Group: Epidemiology, patterns of care, and mortality for patients with acute respiratory distress syndrome in intensive care units in 50 countries. JAMA 2016; 315:788–800
2. Putensen C, Zech S, Wrigge H, Zinserling J, Stüber F, Von Spiegel T, Mutz N: Long-term effects of spontaneous breathing during ventilatory support in patients with acute lung injury. Am J Respir Crit Care Med 2001; 164:43–9
3. Hansen-Flaschen JH, Brazinsky S, Basile C, Lanken PN: Use of sedating drugs and neuromuscular blocking agents in patients requiring mechanical ventilation for respiratory failure. A national survey. JAMA 1991; 266:2870–5
4. Pellegrini M, Hedenstierna G, Roneus A, Segelsjö M, Larsson A, Perchiazzi G: The diaphragm acts as a brake during expiration to prevent lung collapse. Am J Respir Crit Care Med 2017; 195:1608–16
5. Yoshida T, Fujino Y, Amato MB, Kavanagh BP: Fifty years of research in ARDS. Spontaneous breathing during mechanical ventilation. Risks, mechanisms, and management. Am J Respir Crit Care Med 2017; 195:985–92
6. Pelosi P, Rocco PR: Effects of mechanical ventilation on the extracellular matrix. Intensive Care Med 2008; 34:631–9
7. Brochard L, Slutsky A, Pesenti A: Mechanical ventilation to minimize progression of lung injury in acute respiratory failure. Am J Respir Crit Care Med 2017; 195:438–42
8. Yoshida T, Torsani V, Gomes S, De Santis RR, Beraldo MA, Costa EL, Tucci MR, Zin WA, Kavanagh BP, Amato MB: Spontaneous effort causes occult pendelluft during mechanical ventilation. Am J Respir Crit Care Med 2013; 188:1420–7
9. Kallet RH, Alonso JA, Luce JM, Matthay MA: Exacerbation of acute pulmonary edema during assisted mechanical ventilation using a low-tidal volume, lung-protective ventilator strategy. Chest 1999; 116:1826–32
10. Loring SH, Topulos GP, Hubmayr RD: Transpulmonary pressure: The importance of precise definitions and limiting assumptions. Am J Respir Crit Care Med 2016; 194:1452–7

11. Kilkenny C, Browne WJ, Cuthill IC, Emerson M, Altman DG: Improving bioscience research reporting: The ARRIVE guidelines for reporting animal research. PLoS Biol 2010; 8:e1000412
12. Magalhães PAF, Padilha GA, Moraes L, Santos CL, Maia LA, Braga CL, Duarte MDCMB, Andrade LB, Schanaider A, Capellozzi VL, Huhle R, Gama de Abreu M, Pelosi P, Rocco PRM, Silva PL: Effects of pressure support ventilation on ventilator-induced lung injury in mild acute respiratory distress syndrome depend on level of positive end-expiratory pressure: A randomised animal study. Eur J Anaesthesiol 2018; 35:298–306
13. Mortola JP, Noworaj A: Two-sidearm tracheal cannula for respiratory airflow measurements in small animals. J Appl Physiol Respir Environ Exerc Physiol 1983; 55(1 Pt 1):250–3
14. Baydur A, Behrakis PK, Zin WA, Jaeger M, Milic-Emili J: A simple method for assessing the validity of the esophageal balloon technique. Am Rev Respir Dis 1982; 126:788–91
15. Moraes L, Santos CL, Santos RS, Cruz FF, Saddy F, Morales MM, Capelozzi VL, Silva PL, de Abreu MG, Garcia CS, Pelosi P, Rocco PR: Effects of sigh during pressure control and pressure support ventilation in pulmonary and extrapulmonary mild acute lung injury. Crit Care 2014; 18:474
16. Thille AW, Lyazidi A, Richard JC, Galia F, Brochard L: A bench study of intensive-care-unit ventilators: New *versus* old and turbine-based *versus* compressed gas-based ventilators. Intensive Care Med 2009; 35:1368–76
17. Richard JC, Carlucci A, Breton L, Langlais N, Jaber S, Maggiore S, Fougère S, Harf A, Brochard L: Bench testing of pressure support ventilation with three different generations of ventilators. Intensive Care Med 2002; 28:1049–57
18. Henzler D, Dembinski R, Bensberg R, Hochhausen N, Rossaint R, Kuhlen R: Ventilation with biphasic positive airway pressure in experimental lung injury. Influence of transpulmonary pressure on gas exchange and haemodynamics. Intensive Care Med 2004; 30:935–43
19. Bellani G, Grasselli G, Teggia-Droghi M, Mauri T, Coppadoro A, Brochard L, Pesenti A: Do spontaneous and mechanical breathing have similar effects on average transpulmonary and alveolar pressure? A clinical crossover study. Crit Care 2016; 20:142
20. Zakynthinos SG, Vassilakopoulos T, Zakynthinos E, Mavrommatis A, Roussos C: Contribution of expiratory muscle pressure to dynamic intrinsic positive end-expiratory pressure: Validation using the Campbell diagram. Am J Respir Crit Care Med 2000; 162:1633–40
21. Uhlig C, Silva PL, Ornellas D, Santos RS, Miranda PJ, Spieth PM, Kiss T, Kasper M, Wiedemann B, Koch T, Morales MM, Pelosi P, de Abreu MG, Rocco PR: The effects of salbutamol on epithelial ion channels depend on the etiology of acute respiratory distress syndrome but not the route of administration. Respir Res 2014; 15:56
22. Hsia CC, Hyde DM, Ochs M, Weibel ER; ATS/ERS Joint Task Force on Quantitative Assessment of Lung Structure: An official research policy statement of the American Thoracic Society/European Respiratory Society: Standards for quantitative assessment of lung structure. Am J Respir Crit Care Med 2010; 181:394–418
23. Parameswaran H, Majumdar A, Ito S, Alencar AM, Suki B: Quantitative characterization of airspace enlargement in emphysema. J Appl Physiol (1985) 2006; 100:186–93
24. Wierzchon CGRS, Padilha G, Rocha NN, Huhle R, Coelho MS, Santos CL, Santos RS, Samary CS, Silvino FRG, Pelosi P, Gama de Abreu M, Rocco PRM, Silva PL: Variability in tidal volume affects lung and cardiovascular function differentially in a rat model of experimental emphysema. Front Physiol 2017; 8:1071
25. Yoshida T, Uchiyama A, Matsuura N, Mashimo T, Fujino Y: The comparison of spontaneous breathing and muscle paralysis in two different severities of experimental lung injury. Crit Care Med 2013; 41:536–45
26. Matute-Bello G, Downey G, Moore BB, Groshong SD, Matthay MA, Slutsky AS, Kuebler WM; Acute Lung Injury in Animals Study Group: An official American Thoracic Society workshop report: Features and measurements of experimental acute lung injury in animals. Am J Respir Cell Mol Biol 2011; 44:725–38
27. Ferguson ND, Fan E, Camporota L, Antonelli M, Anzueto A, Beale R, Brochard L, Brower R, Esteban A, Gattinoni L, Rhodes A, Slutsky AS, Vincent JL, Rubenfeld GD, Thompson BT, Ranieri VM: The Berlin definition of ARDS: An expanded rationale, justification, and supplementary material. Intensive Care Med 2012; 38:1573–82
28. Saddy F, Sutherasan Y, Rocco PR, Pelosi P: Ventilator-associated lung injury during assisted mechanical ventilation. Semin Respir Crit Care Med 2014; 35:409–17
29. Yoshida T, Engelberts D, Otulakowski G, Katira B, Post M, Ferguson ND, Brochard L, Amato MBP, Kavanagh BP: Continuous negative abdominal pressure reduces ventilator-induced lung injury in a porcine model. Anesthesiology 2018; 129:163–72
30. Yoshida T, Engelberts D, Otulakowski G, Katira B, Ferguson ND, Brochard L, Amato MBP, Kavanagh BP: Continuous negative abdominal pressure: Mechanism of action and comparison with prone position. J Appl Physiol (1985) 2018; 125:107–16
31. Chierichetti M, Engelberts D, El-Khuffash A, Babyn P, Post M, Kavanagh BP: Continuous negative abdominal distension augments recruitment of atelectatic lung. Crit Care Med 2012; 40:1864–72

32. Engelberts D, Malhotra A, Butler JP, Topulos GP, Loring SH, Kavanagh BP: Relative effects of negative *versus* positive pressure ventilation depend on applied conditions. Intensive Care Med 2012; 38:879–85
33. Esteban A, Frutos-Vivar F, Muriel A, Ferguson ND, Peñuelas O, Abraira V, Raymondos K, Rios F, Nin N, Apezteguía C, Violi DA, Thille AW, Brochard L, González M, Villagomez AJ, Hurtado J, Davies AR, Du B, Maggiore SM, Pelosi P, Soto L, Tomicic V, D'Empaire G, Matamis D, Abroug F, Moreno RP, Soares MA, Arabi Y, Sandi F, Jibaja M, Amin P, Koh Y, Kuiper MA, Bülow HH, Zeggwagh AA, Anzueto A: Evolution of mortality over time in patients receiving mechanical ventilation. Am J Respir Crit Care Med 2013; 188:220–30
34. Marini JJ, Jaber S: Dynamic predictors of VILI risk: Beyond the driving pressure. Intensive Care Med 2016; 42:1597–600
35. Protti A, Andreis DT, Monti M, Santini A, Sparacino CC, Langer T, Votta E, Gatti S, Lombardi L, Leopardi O, Masson S, Cressoni M, Gattinoni L: Lung stress and strain during mechanical ventilation: any difference between statics and dynamics? Crit Care Med 2013; 41:1046–55
36. Moriondo A, Mukenge S, Negrini D: Transmural pressure in rat initial subpleural lymphatics during spontaneous or mechanical ventilation. Am J Physiol Heart Circ Physiol 2005; 289:H263–9
37. Hedenstierna G, Lattuada M: Lymphatics and lymph in acute lung injury. Curr Opin Crit Care 2008; 14:31–6
38. Futier E, Constantin JM, Combaret L, Mosoni L, Roszyk L, Sapin V, Attaix D, Jung B, Jaber S, Bazin JE: Pressure support ventilation attenuates ventilator-induced protein modifications in the diaphragm. Crit Care 2008; 12:R116
39. McClung JM, Kavazis AN, DeRuisseau KC, Falk DJ, Deering MA, Lee Y, Sugiura T, Powers SK: Caspase-3 regulation of diaphragm myonuclear domain during mechanical ventilation-induced atrophy. Am J Respir Crit Care Med 2007; 175:150–9
40. Casetti AV, Bartlett RH, Hirschl RB: Increasing inspiratory time exacerbates ventilator-induced lung injury during high-pressure/high-volume mechanical ventilation. Crit Care Med 2002; 30: 2295–9
41. Rich PB, Reickert CA, Sawada S, Awad SS, Lynch WR, Johnson KJ, Hirschl RB: Effect of rate and inspiratory flow on ventilator-induced lung injury. J Trauma 2000; 49:903–11
42. Garcia CS, Abreu SC, Soares RM, Prota LF, Figueira RC, Morales MM, Capelozzi VL, Zin WA, Rocco PR: Pulmonary morphofunctional effects of mechanical ventilation with high inspiratory air flow. Crit Care Med 2008; 36:232–9
43. Yoshida T, Amato MBP, Grieco DL, Chen L, Lima CAS, Roldan R, Morais CCA, Gomes S, Costa ELV, Cardoso PFG, Charbonney E, Richard JM, Brochard L, Kavanagh BP: Esophageal manometry and regional transpulmonary pressure in lung injury. Am J Respir Crit Care Med 2018; 197:1018–26